Extreme Temperature Operation of Ultra-Wide Bandgap AlGaN High Electron Mobility Transistors

Patrick H. Carey, IV, Fan Ren, *Fellow, IEEE*, Albert G. Baca, Brianna A. Klein, Andrew A. Allerman, Andrew M. Armstrong, Erica A. Douglas, Robert J. Kaplar, *Senior Member, IEEE*, Paul G. Kotula, and Stephen J. Pearton, *Fellow, IEEE*

***Abstract*—High Aluminum content channel ($Al_{0.85}Ga_{0.15}N$/$Al_{0.7}Ga_{0.3}N$) High Electron Mobility Transistors (HEMTs) were operated from room temperature to 500°C in ambient. The devices exhibited only moderate reduction, 58%, in on-state forward current. Gate lag measurements at 100 kHz and 10% duty only showed a slight reduction in pulsed current from DC at 500°C and high gate voltages. Interfacial trap densities were 2×10^{11} over the range 25-300°C and 3×10^{12} cm^{-2} from 300-500°C from the subthreshold swing. These low interfacial trap densities and the near ideal gate lag measurement indicate high-quality epi layers. The insulating properties of the barrier layer led to low gate induced drain leakage current of $\sim 10^{-12}$ A/mm and $\sim 10^{-8}$ A/mm at 25 and 500°C, respectively. Low leakage current was enabled by the high Schottky barrier of the Ni/Au gate, 1.1 eV and 3.3 eV at 25 and 500°C, respectively. These properties of the AlGaN channel HEMTs demonstrate their potential for high power and high temperature operation.**

***Index Terms*—AlGaN, GaN, high electron mobility transistor (HEMT), high temperature.**

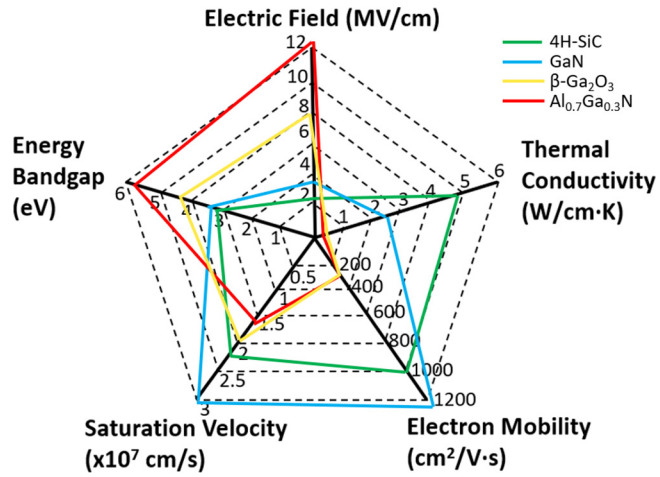

Fig. 1. Comparison of 4H-SiC, GaN, β-Ga_2O_3, and $Al_{0.7}Ga_{0.3}N$ critical electric field, thermal conductivity, electron mobility, saturation velocity and energy bandgap.

I. Introduction

THE MATERIALS of choice for power semiconductors have become SiC and GaN for their superior material properties in high frequency and high power applications. The primary limitations of GaN and SiC technologies are the critical breakdown electric field, E_c, and energy densities. The E_c of SiC (2.5 MV/cm) and GaN (3.9 MV/cm) are an improvement over their Si competitors (0.3 MV/cm) but can be improved further in GaN with the shift to high aluminum content channel HEMTs. These new devices are now termed "ultra" wide bandgap materials (UWBG), which encompasses any material with a bandgap greater than GaN (3.4 eV). The primary UWBG materials receiving much interest have been β-Ga_2O_3 (4.7 eV), diamond (5.5 eV), and AlN (6.2 eV). Each of these materials presents their own set of growth, processing, and operating difficulties. A key benefit of shifting to AlGaN HEMTs is much of the previous work on GaN HEMTs can be applied, albeit reinterpreted and reoptimized.

The primary difficulty with AlGaN channel HEMTs is realizing high quality Ohmic contacts. The primary approaches have utilized regrowth and Si implantation [1]–[4]. With any implanted contact, impurity scattering will lower the high frequency performance and as such can only find limited uses for low frequency switching operation. Additionally, using a ternary material, AlGaN, the thermal conductivity is quite low; however, as growth is performed on AlN substrate, device self-heating can be managed. The benefits of using an AlN substrate also extend to reduced threading dislocations and other growth-related defects as the lattice parameters for $Al_{0.7}Ga_{0.3}N$ are nominally different from AlN.

To better demonstrate the potential for AlGaN HEMTs, a pentagram of material factors is presented in Fig. 1. The advantageous factors that the high aluminum content AlGaN

Manuscript received June 23, 2019; revised July 18, 2019; accepted July 21, 2019. Date of publication July 31, 2019; date of current version October 29, 2019. This work was supported in part by the Laboratory Directed Research and Development program at Sandia, in part by the Sandia National Laboratories is a multi-program laboratory managed and operated by National Technology and Engineering Solutions of Sandia, LLC, a wholly owned subsidiary of Honeywell Corporation, for the U.S. Department of Energy's National Nuclear Security Administration under Contract DE-NA0003525. The work of P. H. Carey, F. Ren, and S. J. Pearton was supported in part by the Department of the Defense, Defense Threat Reduction Agency monitored by Jacob Calkins under Grant HDTRA1-17-1-011. *(Corresponding author: Patrick H. Carey, IV.)*

P. H. Carey, IV, and F. Ren are with the Department of Chemical Engineering, University of Florida, Gainesville, FL 32611 USA (e-mail: careyph@ufl.edu).

A. G. Baca, B. A. Klein, A. A. Allerman, A. M. Armstrong, E. A. Douglas, R. J. Kaplar, and P. G. Kotula are with the Sandia National Laboratories, Albuquerque, NM 87185 USA.

S. J. Pearton is with the Department of Materials Science and Engineering, University of Florida, Gainesville, FL 32611 USA.

Color versions of one or more of the figures in this article are available online at http://ieeexplore.ieee.org.

Digital Object Identifier 10.1109/TSM.2019.2932074

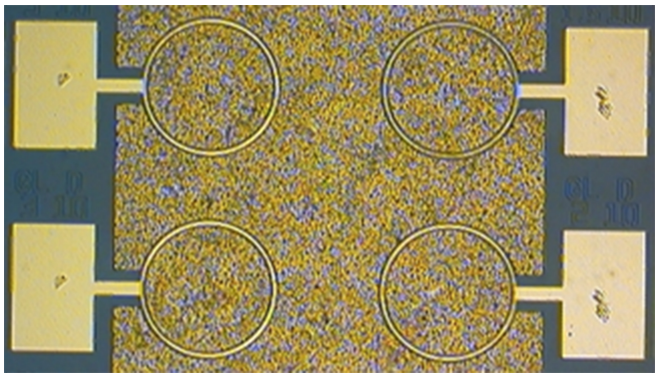

Fig. 2. Optical image of an array of circular HEMT test structures.

can provide are high power and high temperature due to its high bandgap and critical electric field. The mobility is the second drawback, since in using a ternary channel layer, the effects of polarization optical phonon scattering will be significant, especially at elevated temperatures. Even with this intrinsic limitation, successful RF performance for these devices is still attainable [5].

In this manuscript, DC characterization of $Al_{0.85}Ga_{0.15}N/Al_{0.7}Ga_{0.3}N$ (85/70) HEMTs was performed from chuck temperatures of 25-500°C. Pulsed characterization via gate lag was also performed to observe current collapse if a virtual gate were to form. The devices' Schottky barrier height, transconductance, mobility, subthreshold swing, and other parameters were extracted and analyzed.

II. Device Fabrication and Characterization

The HEMT samples were prepared by metal organic chemical vapor deposition (MOCVD) on sapphire substrates. First, a 1.6 μm AlN nucleation and buffer layer were grown on the substrate. Then a transition layer from 100% Al to 70% Al was graded over 50 nm thickness. The 400 nm unintentionally doped channel layer, $Al_{0.7}Ga_{0.3}N$, was grown next, followed by the 25 nm $Al_{0.85}Ga_{0.15}N$ barrier layer. The barrier layer was doped with Si at 3×10^{18} cm^{-3}. Contactless measurement of the 2DEG showed the resistivity to be 2200 Ω/□, combined with capacitance-voltage (CV) measurements showing sheet carrier density $n_s = 9 \times 10^{12}$ cm^{-2}. Circular HEMT devices were fabricated with a gate length of 2 μm, and source/drain to gate spacing of 4 μm. The gate had a circumference at its center of 660 μm. Planar Ohmic contacts (Ti/Al/Ni/Au) were deposited and subsequently annealed. The gate was formed by deposition of Ni/Au into an opening on the 100 nm thick SiN dielectric to allow for edge termination. An optical image of an array of circular FETs is presented in Fig. 2.

DC characterization was carried out using an Agilent 4156C parameter analyzer. A Tektronix Curve Tracer 370A was used to collect high voltage I-V curves. A Wentworth automated temperature control chuck was used to vary the chuck temperature from room temperature to 500°C. A temperature probe and an external IR camera were used to verify the surface of the sample was at the target temperature.

III. Results and Discussion

The current-voltage characteristics of the test devices are shown in Fig. 3 in 100°C increments from room temperature to 500°C. The total peak forward current was reduced from 122 mA/mm to 52 mA/mm from 25 to 500°C, a reduction of 57%. The majority of the current reduction occurred from room temperature to 300°C, accounting for 42%. It is also interesting to note that as the devices are heated, they exhibit increasingly ideal performance, with the output resistance becoming near infinite at high temperatures (horizontal in the saturation regime). At room temperature there was a slightly non-Ohmic behavior in the low field region, as the drain I-V has an almost Schottky-like appearance, but with heating to 100°C, this effect was removed and entirely linear current-voltage characteristics through the origin were obtained. The conduction mechanism above $V_d = +3$ V was primarily mobility- dominated conduction, which is indicated by all applied gate voltages having the same positive slopes in the linear regime.

Fig. 4 shows the linear drain current as a function of gate voltage and the transfer characteristics at 25 and 500°C. Peak extrinsic transconductance of 12.5 mS/mm and 4.7 mS/mm were achieved at these respective temperatures. The threshold voltage extracted from the $\sqrt{I_D}$- V_{gs} method was approximately −2.3 V; however, the device undergoes soft turn-on from −2.3 to 0 V when operated at room temperature, which is indicative of high source and drain contact resistance. At 500°C, the threshold voltage of −2.4 V was extracted using the $\sqrt{I_D}$- V_{gs} method, but as with the current-voltage characteristics, at elevated temperature the contact resistance no longer dominates the low field regime.

The logarithmic I_d-V_g and I_{gg} are presented in Fig. 5. The deep subthreshold voltage was invariant across the temperature range, indicating the 2DEG charge density is fairly constant. Thus, the changes we see in the low field regime (pseudo-Schottky at low temperatures), is primarily due to the Ohmic contact limitations and mobility, not shifts in the threshold voltage. From a design perspective, a nearly constant deep subthreshold voltage is advantageous as pinch-off can be achieved at the same voltage and simplifies operational parameters for full temperature range operation.

From the gate induced drain leakage current (GIDL), the activation energy can be extracted assuming an Arrhenius temperature dependence. Two regimes were noted, 25 to 350°C and 350 to 500°C with $E_a = 0.63$ eV and $E_a = 0.076$ eV, respectively. The $E_a = 0.63$ eV is consistent with trap assisted Poole Frenkel Emission [3]. For GaN channel-based devices this is also the dominant mechanism for < 300°C operation. Once heated above this temperature, GaN devices suffer from bulk excitation contributions. The bandgap of AlGaN (5.4 eV) is significantly higher than GaN (3.4 eV) to avoid this in our devices. For the 350 to 500°C range, the $E_a = 0.076$ eV value is consistent with band-to-band tunneling and does not rely on mid-gap states. Additionally, it is interesting to note that under

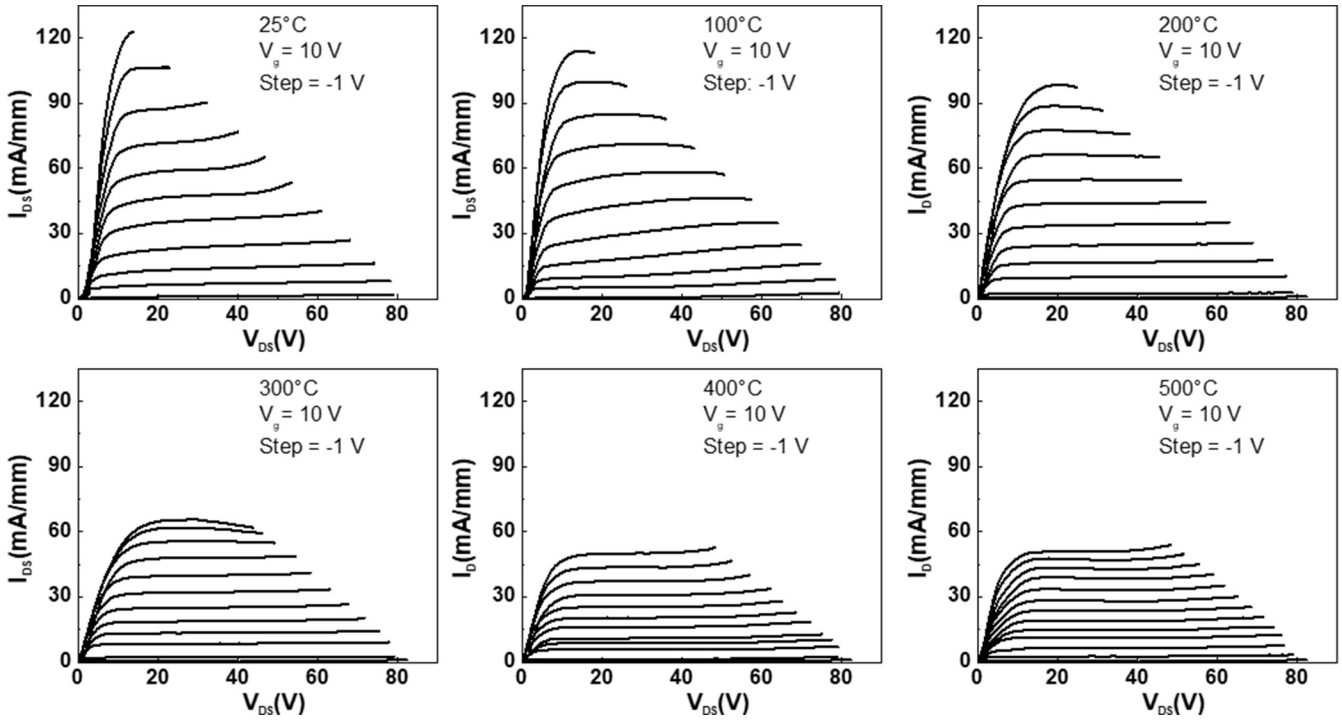

Fig. 3. I-V characteristic curves from 25 to 500°C in 100°C increments.

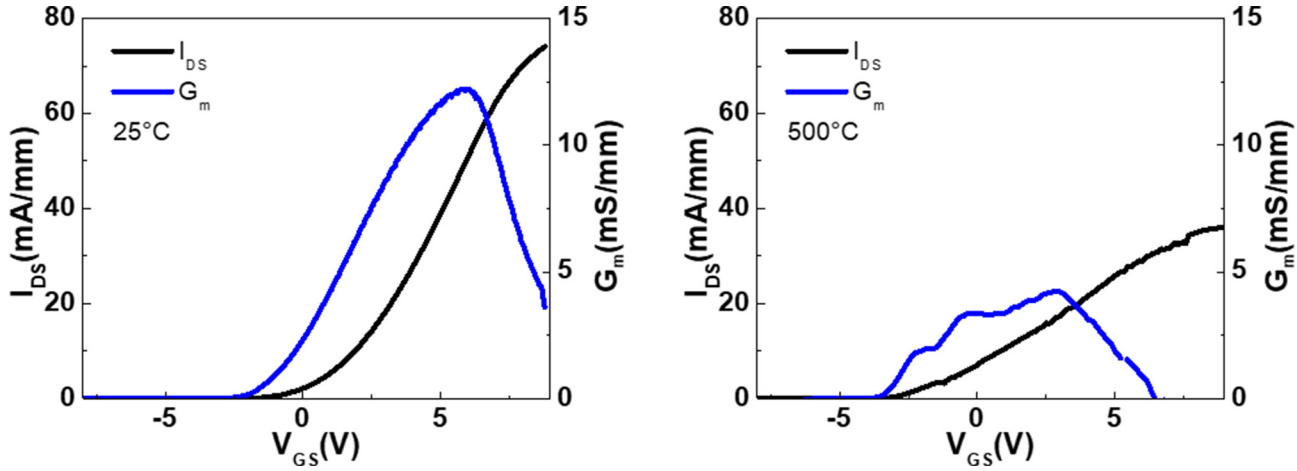

Fig. 4. Transfer characteristics at room temperature and 500°C under $V_d = +10$ V.

a drain bias the gate is able to enhance current flow up to +10V, even though the device is depletion mode. Traditional n-GaN devices are unable to operate at such high gate voltages due to excessive gate leakage current. For the 85/70 material system, the highly insulator like 85% Al barrier layer leads to this ability.

To further understand the gate characteristics, the thermionic emission model was used to measure the zero bias Schottky barrier height and ideality factor as a function of temperature, Fig. 6. A comparison is shown between a traditional GaN HEMT ($Al_{0.26}Ga_{0.74}N$/GaN) device with a Ni/Au gate and our high-Al HEMTs. The GaN device barrier height is subject to some surface pinning effects as it lacks a significant temperature dependence. For the case of the 85/70 channel device, the barrier height is not subject to surface pinning and increases from 1.2 eV to 3.3 eV at 25 and 500°C, respectively. This significant shift in barrier height enables controlled modulation of drain current at high temperatures and prevents excessive leakage current. The primary drawback when using Ni/Au is the metal atoms becoming mobile and intermixing when heated above 350°C. As such, the devices would undergo a permanent change when operated above 350°C and could not recover their initial state characteristics. This is a subject of our future studies to introduce diffusion barrier layers and the use of refractory metals for improved stability of the gate contact.

One of the primary benefits of GaN HEMT is the formation of a high mobility 2D electron gas (2DEG) enabling high frequency operation. A drawback of GaN HEMT is the mobility degrades by several orders of magnitude from 25 to 500°C,

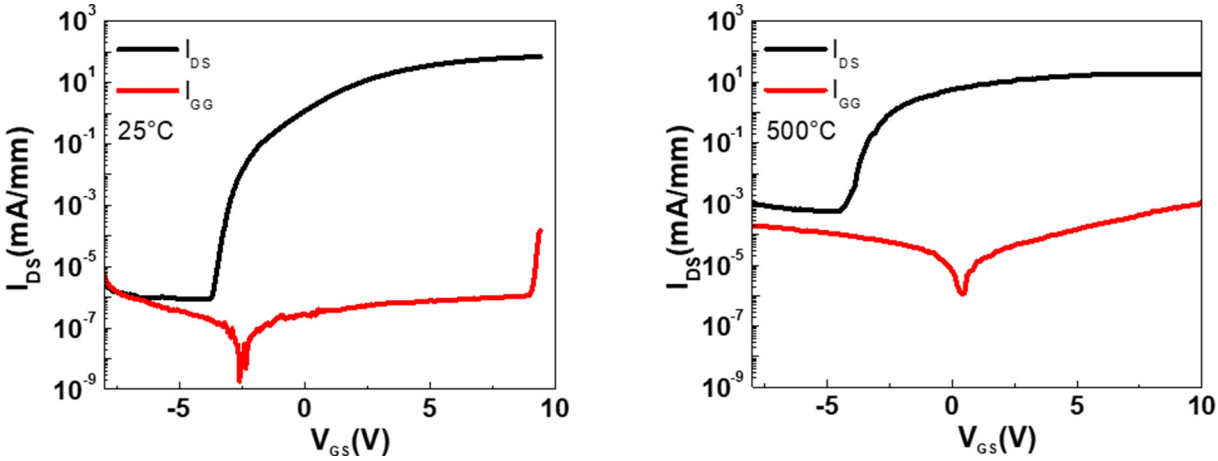

Fig. 5. Logarithmic I_d-V_g and I_{gg} at 25 and 500°C under $V_d = +10$ V.

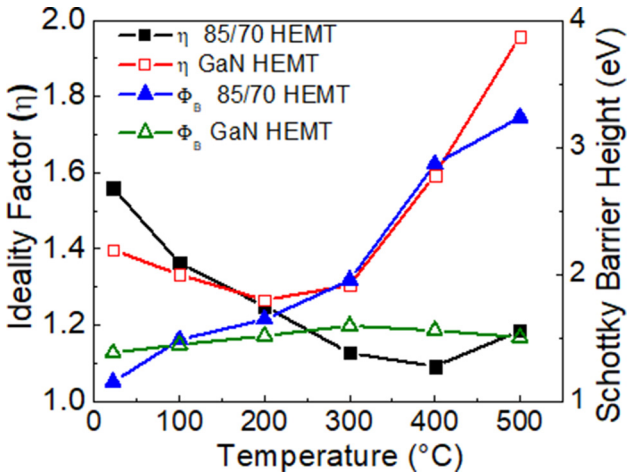

Fig. 6. Ideality Factor and Schottky Barrier Height as a function of temperature for the 85/70 and GaN HEMT.

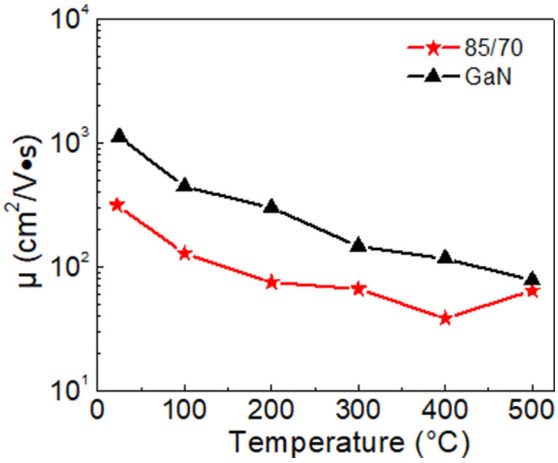

Fig. 7. Electron mobility as a function of temperature for the 85/70 and GaN HEMT.

Fig. 7. The 85/70 HEMT does not suffer from the same amount of mobility reduction at elevated temperatures. However, the room temperature mobility of the 85/70 HEMT is significantly lower than conventional GaN HEMTs. This is primarily due to the issue of using a ternary channel layer. The effects of polar optical phonon scattering for AlGaN at elevated temperatures dominate the mobility and will limit performance [6].

To evaluate the ideality of these devices under low frequency switching operation, gate lag measurements were performed. The device drain is held under a constant bias of +10 V, while the gate is switched at 100 kHz and 10% duty from −6V to the operating voltage, Fig. 7. While this is higher frequency than standard operational power switching, it is useful to push the devices to the extreme and observe the trapping characteristics and formation of a virtual gate under such conditions.

At room temperature there is no formation of a virtual gate, and only with heating and under high gate voltages is any formation of a virtual gate noted. This near-ideal performance demonstrates both the quality of the epitaxial layers growth and potential for power switching.

Another metric for the ideality of these devices is the subthreshold slope, which was extracted from the I_d-V_g curves. For room temperature operation, 88 mV/dec was measured and is near the ideal subthreshold slope of 60 mV/dec. At 500°C the value has increased to 242 mV/dec while the ideal is 152 mV/dec, Fig. 8. The heterointerfacial trap density can be extracted from the differential of subthreshold slope and trap density with respect to temperature:

$$\frac{dS}{dT} = \frac{kT}{q}\ln(10)\left(1 + \frac{D_{it}q}{C_{AlGaN}}\right)$$

where S is the subthreshold slope, T is temperature, k, is the Boltzmann constant, q is the charge of an electron, C_{AlGaN} is the capacitance of the barrier layer, and D_{it} is the interfacial trap density. The benefit of using the differentiated form is the reduction in error. However, trap density can vary widely depending on methodology. Two linear regimes were noted for the subthreshold swing, 25 to 300°C and 300 to 500°C with trap densities of 2×10^{11} cm^{-2} and 3×10^{12} cm^{-2}, respectively. This behavior is expected as the thermal energy is sufficient to activate and detrap electrons.

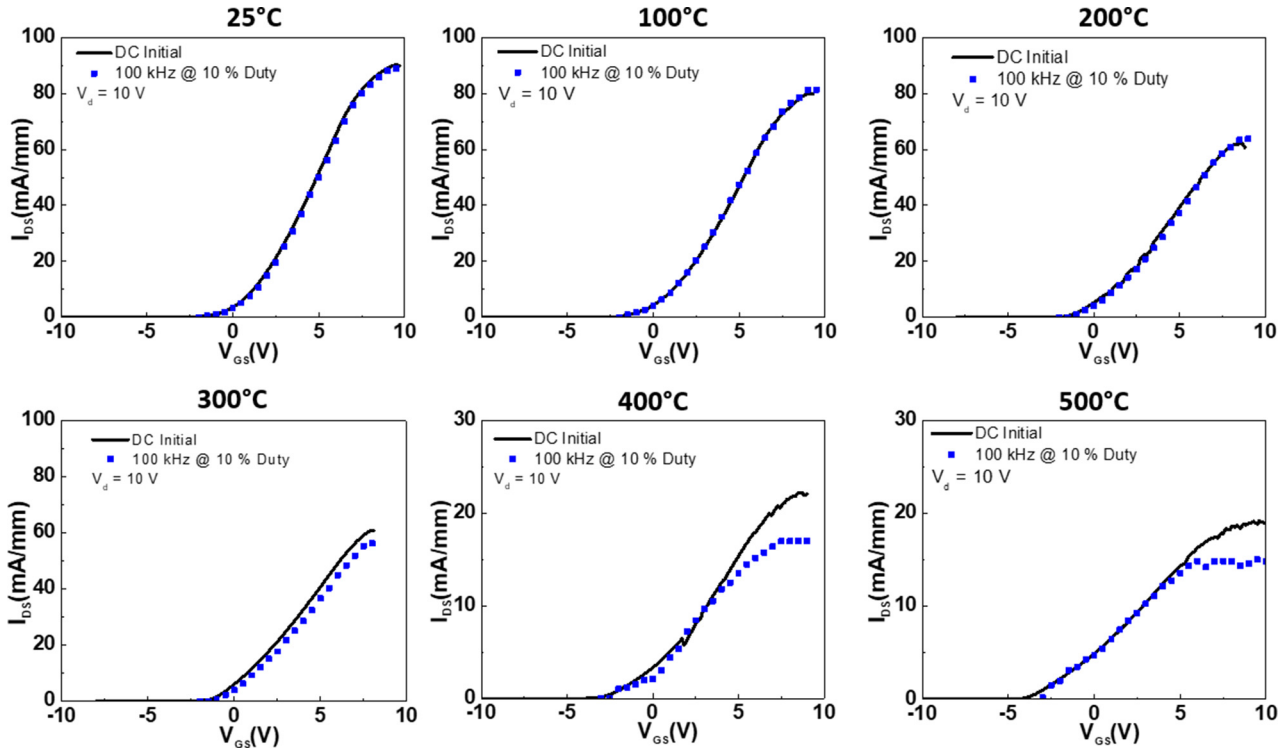

Fig. 8. Gate lag measurements from 25 to 500°C in 100°C increments.

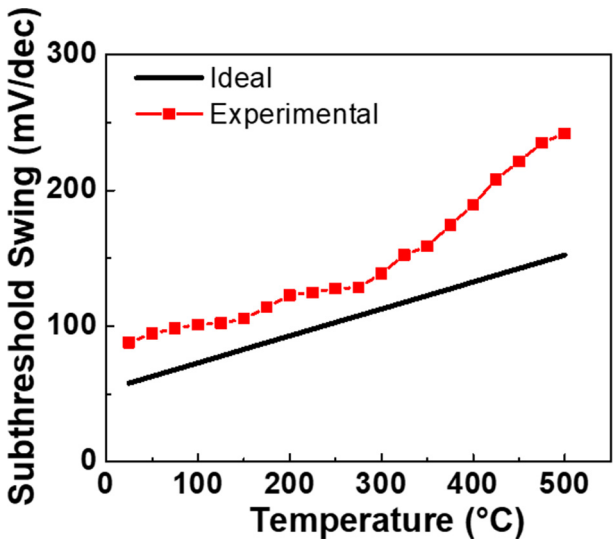

Fig. 9. Temperature dependence of the subthreshold slope from 25 to 500°C for test device and ideal case.

IV. Conclusion

In summary, $Al_{0.85}Ga_{0.15}N/Al_{0.7}Ga_{0.3}N$ high electron mobility transistors have been characterized and operated from 25 to 500°C in ambient atmosphere. The forward current was reducted 58% across this temperature range, and the gate provided full modulation and pinchoff regardless of temperature. The Ni/Au gate's unpinned barrier height enabled this excellent high temperature operation but the metal contact showed some reordering. The low gate leakage current lead to excellent on/off ratios of 2×10^{11} and 3×10^{6} at 25 and 500°C, respectively. The near ideal switching performance indicates the potential for this material system to succeed in high power and high temperature applications, greatly mitigating cooling costs that would normally be required. The primary limiting factor for this technology is the current state of the Ohmic contacts; however, as we are early in this materials development cycle, this issue may be mitigated in future works.

Acknowledgment

This paper describes objective technical results and analysis. Any subjective views or opinions that might be expressed in the paper do not necessarily represent the views of the U.S. Department of Energy or the United States Government.

References

[1] T. Nanjo *et al.*, "First operation of AlGaN channel high electron mobility transistors," *Appl. Phys. Exp.*, vol. 1, no. 1, 2007, Art. no. 011101. doi: 10.1143/APEX.1.011101.

[2] M. Hatano *et al.*, "Comparative high-temperature DC characterization of HEMTS with GaN and AlGaN channel layers," in *Proc. CS MANTECH Conf.*, Portland, OR, USA, May 2010, p. 101.

[3] A. Baca *et al.*, "$Al_{0.85}Ga_{0.15}N/Al_{0.70}Ga_{0.30}N$ high electron mobility transistors with Schottky gates and large on/off current ratio over temperature," *ECS Journal of Solid State Science and Technology*, vol. 6, no. 12, pp. Q161–Q165, 2017. doi: 10.1149/2.0231712jss.

[4] P. Carey *et al.*, "Extreme temperature operation of ultra-wide bandgap AlGaN high electron mobility transistors," in *Proc. CS MANTECH Conf.*, Minneapolis, MN, USA, Apr./May 2019, pp. 191–194.

[5] A. G. Baca *et al.*, "RF performance of $Al_{0.85}Ga_{0.15}N/Al_{0.70}Ga_{0.30}N$ high electron mobility transistors with 80-nm gates," *IEEE Electron Device Lett.*, vol. 40, no. 1, pp. 17–20, Jan. 2019. doi: 10.1109/LED.2018.2880429.

[6] P. H. Carey *et al.*, "Operation up to 500 °C of $Al_{0.85}Ga_{0.15}N/Al_{0.7}Ga_{0.3}N$ high electron mobility transistors," *IEEE J. Electron Devices Soc.*, vol. 7, pp. 444–452, Mar. 2019. doi: 10.1109/JEDS.2019.2907306.